Biochimica et Biophysica Acta 1808 (2011) 209–218

Contents lists available at ScienceDirect

Biochimica et Biophysica Acta

journal homepage: www.elsevier.com/locate/bbamem

Kinetic analysis of the interaction between poly(amidoamine) dendrimers and model lipid membranes

Venkataswarup Tiriveedhi [a,1], Kelly M. Kitchens [b], Kerrick J. Nevels [b], Hamidreza Ghandehari [c], Peter Butko [b,*]

[a] Department of Chemistry & Biochemistry, University of Southern Mississippi, Hattiesburg, MS 39406, USA
[b] Department of Pharmaceutical Sciences, University of Maryland School of Pharmacy, Baltimore, MD 21201, USA
[c] Departments of Pharmaceutics & Pharmaceutical Chemistry and Bioengineering, Utah Center for Nanomedicine, Nano Institute of Utah, University of Utah, 383 Colorow Road, Room 343, Salt Lake City, UT 84108, USA

ARTICLE INFO

Article history:
Received 26 May 2010
Received in revised form 11 August 2010
Accepted 24 August 2010
Available online 7 September 2010

Keywords:
Cell-penetrating molecules
Fluorescence spectroscopy
Membrane fluidity
PAMAM dendrimers
Quenching
Resonance energy transfer

ABSTRACT

We used fluorescence spectroscopy and surface tensiometry to study the interaction between low-generation (G1 and G4) poly(amidoamine) (PAMAM) dendrimers, potential vehicles for intracellular drug delivery, and model lipid bilayers. Membrane association of fluorescently labeled dendrimers, measured by fluorescence anisotropy, increased with increasing size of the dendrimer and with increasing negative charge density in the membrane, indicating the electrostatic nature of the interaction. When the membrane was doped with pyrene-labeled phosphatidyl glycerol (pyrene-PG), pyrene excimer fluorescence demonstrated a dendrimer-induced selective aggregation of negatively charged lipids when the membrane was in the liquid crystalline state. A nonlinear Stern–Volmer quenching of dendrimer fluorescence with cobalt bromide suggested a dendrimer-induced aggregation of lipid vesicles, which increased with the dendrimer's generation number. Surface tensiometry measurements showed that dendrimers penetrated into the lipid monolayer only at subphysiologic surface pressures (<30 mN/m). We conclude that the low-generation PAMAM dendrimers associate with lipid membranes predominantly electrostatically, without significantly compromising the bilayer integrity. They bind stronger to membranes with higher fluidity and lower surface pressure, which are characteristic of rapidly dividing cells.

1. Introduction

Dendrimers, highly branched complex macromolecules were discovered in early 1980s [1,2]. Poly(amidoamine) (PAMAM) dendrimers with amino termini, also called star-burst dendrimers, were first synthesized dendrimers that extended up to 10 generations [3,4]. They can be prepared by either convergent or divergent methods, with an exponential increase in the number of charged groups on the molecule's surface [5]. Their molecular shape depends on the generation number: lower-generation dendrimers (G4 and below) have an ellipsoidal shape and open, porous structures, while higher-generation dendrimers (G5 and above) are spherical and have a closed-shell structure [6]. Unlike the classical polymerization, which produces linear polymers of different sizes, dendrimer size can be specifically controlled during the synthesis. Dendrimers can be loaded with cargo molecules by trapping small molecules inside the "dendritic box" or by forming covalent linkage with their terminal amino groups [7]. Due to their high water solubility and unique interior structure, dendrimers have been of particular interest in the biomedical field as potential intracellular drug delivery vehicles [8–10]: they have been shown to transfer DNA fragments [11–14], immunoglobulins [15], and anticancer drugs [16] across the cell membrane. Importantly, PAMAM dendrimers have been shown to be capable of traversing the intestinal epithelial barrier, thereby rendering the dendrimer system uniquely suitable for applications in oral drug delivery [17–19].

In general, all cell-penetrating macromolecules are cationic at physiologic pH [20]. From physicochemical point of view, it is intriguing that these relatively large and highly charged molecules can cross the hydrophobic core of the lipid bilayer. As with cell-penetrating peptides such as TAT-PTD [21], the exact mechanism of dendrimer entry is yet to be established. Several theories, such as adsorptive endocytosis [22,23], inverted-micelle formation [24], and membrane hole formation [25], have been proposed. The major forces driving the interaction in cell-penetrating systems are thought to be both electrostatic and hydrophobic, which eventually lead to osmotic imbalance [26]. However, there is a considerable variation in molecular structures and shapes of cell-penetrating macromolecules,

* Corresponding author. Department of Pharmaceutical Sciences, University of Maryland School of Pharmacy, 20 N. Pine St., PH 515, Baltimore, MD 21201, USA. Tel.: +1 410 706 8521; fax: +1 425 696 9603, +1 410 706 0346.
E-mail address: pbutko@rx.umaryland.edu (P. Butko).
[1] Present address: Department of Surgery-Box 8109, Washington University School of Medicine, 660 S. Euclid Avenue, St. Louis, MO, USA.

0005-2736/$ – see front matter © 2010 Elsevier B.V. All rights reserved.
doi:10.1016/j.bbamem.2010.08.017

which makes one single mechanism of action for all these molecules improbable [20].

The promise of PAMAM dendrimers as potential intracellular drug delivery vehicles [9,10] has drawn a lot of attention to this field. Despite much effort, molecular details of dendrimers' entry into cells are not clear. Thermodynamically, it is hard for a large cationic dendrimer to pass directly through the hydrophobic core of the lipid bilayer. Even if that were somehow possible, cell membrane integrity would most probably suffer in the course of the dendrimer passage. Indeed, the cytotoxic effect of higher-generation dendrimers was detected by a substantial release of entrapped calcein from lipid vesicles [12,23]. This fact points to the need for more *in vitro* research before progressing to dendrimers' biological/medical applications.

Leakage studies by several authors showed an increased membrane disruption with higher-generation [13,23,25]. Parimi et al. [27] have studied dendrimer interactions with supported lipid bilayers by optical waveguide lightmode spectroscopy and atomic force microscopy. They observed complex kinetics with the opposite dependence on dendrimer generation in two processes: dendrimer adsorption to the lipid decreased, whereas, in agreement with the previous literature, membrane disruption increased, with increasing generation number. More recently Parimi et al. extended their work to studies of dendrimer cytotoxicity in two cell lines, [28]. Their observations suggest that lower-generation dendrimers are less harmful to the HEK293T and HeLa cells. This is the case for many other cell lines [17,29,30], even though the extent of membrane damage depends on cell type and dendrimer generation [31]. For this reason, lower-generation dendrimers are more promising as potential therapeutic vehicles and nonviral transfection agents [32,33].

In this work we solely focus on the first phase of the interaction of dendrimers with membranes, which is binding of the dendrimer to the free (that is, unsupported) lipid bilayer. We used fluorescence spectroscopy and surface tensiometry to quantitatively describe the interaction of low-generation dendrimers G1 and G4 with the lipid bilayer and monolayer. SUV are the preferred membrane model for fluorescence spectroscopy studies because, despite some drawbacks, such as higher surface curvature and membrane strain, and lower long-term stability, SUV exhibit lower light scattering, when compared to multilamellar and large or giant unilamelar vesicles. Employment of an in vitro system allowed us to rigorously study effects of variables such as the presence of anionic lipids in the membrane or of salt in the external environment, membrane fluidity and surface pressure, etc., which are either ill defined or difficult to control in biological systems.

2. Materials and methods

2.1. Materials

Unlabelled, approximately 90% monodisperse (according to the manufacturer) G1 (MW 1,428) and G4 (MW 14,215) PAMAM dendrimers, fluorescein isothiocyanate (FITC), Oregon green, and egg PC (L-α-phosphatidylcholine) were obtained from Sigma-Aldrich. Lipids egg PG (L-α-phosphatidylglycerol), DMPC (1,2-dimyristoyl-*sn*-glycero-3-phosphocholine), DMPG (1,2-dimyristoyl-*sn*-glycero-3-[phospho-rac-(1-glycerol)]), and rhodamine-PE (1,2-dioleoyl-*sn*-glycero-3-phosphoethanolamine-N-(lissamine rhodamine B sulfonyl), ammonium salt) were from Avanti Polar Lipids (Alabaster, AL). Pyrene-PG (1-hexadecanoyl-2-(1-pyrenedecanoyl)-*sn*-glycero-3-phosphoglycerol) and calcein were purchased from Invitrogen-Molecular Probes (Carlsbad, CA). Cobalt (II) bromide was from Research Organic/Inorganic Chemical Co. (Sun Valley, CA). Buffers, salts, and HPLC-grade water were from either Fisher Scientific (Pittsburgh, PA) or VWR (Atlanta, GA). HEPES buffer contained 10 mM HEPES and 150 mM NaCl, pH adjusted to 7.4.

2.2. Fluorescence labeling of dendrimers

PAMAM dendrimers were fluorescently labeled as previously described [19]. G1 and G4 dendrimers were conjugated to FITC or Oregon-green at a feed molar ratio of 1:1. Fluorescently labeled dendrimers were purified by dialysis against distilled water using dialysis membranes of 500 MWCO (Spectrum Laboratories, Inc., Rancho Dominguez, CA). They were then fractionated on a Superose 12 HR 16/50 preparative column using a Fast Protein Liquid Chromatography (FPLC) system (Amersham Pharmacia Biotech, Uppsala, Sweden) with a mobile phase of 30%/70% (v/v) acetonitrile/Tris buffer (pH 8.0) at a flow rate of 1.0 ml/min. Fractions corresponding to the appropriate dendrimer size and molecular weight were collected, dialyzed against distilled water, and lyophilized. The extent of labeling was determined from absorption spectra collected with Ultrospec 4000 UV-vis spectrophotometer (Biochrom Ltd., Cambridge, UK).

2.3. Vesicle preparation

Small unilamellar vesicles (SUV) were prepared by sonication [21]. Desired amounts of lipids were dissolved in chloroform and dried under a stream of nitrogen. The resulting dry thin film was hydrated in 0.5 ml buffer, so that the stock concentration of lipid was 13 mM. This lipid suspension was sonicated for 30 min (PC vesicles) or 10 min (PG-containing vesicles) at 4 °C with Sonic Dismembrator-Model 300 from Fisher Scientific. For calcein-loaded SUV, calcein was dissolved in distilled water and pH adjusted to 7.4. The lipid suspension was sonicated as described above and the unentrapped calcein was removed by passing 0.1 mL of the SUV suspension through Sephadex G-25 column (1 cm × 30 cm), eluted with HEPES buffer. The nominal calcein concentration in solution to hydrate the lipid film was 80 mM. The efficiency of calcein entrapment in SUV was not experimentally determined in this study, but historically, it has been about 85% to 90% in our laboratory (unpublished data). Based on the preparation method used and literature data [34,35], the average diameter of our SUV is estimated as 25–35 nm.

2.4. Fluorescence and absorption spectra

Fluorescence measurements were performed with an ISS K2 fluorometer (Champaign, IL) equipped with a xenon lamp, variable slits, and a microprocessor-controlled photomultiplier. Samples were measured in 1 cm × 1 cm or 0.3 cm × 0.3 cm quartz cuvettes with adequate stirring. The excitation and emission wavelengths were, respectively, 490 nm and 520 nm for calcein, 490 nm and 525 nm for FITC, 490 nm and 528 nm for Oregon green, 340 nm and 400 nm (475 nm for excimer) for pyrene, and 540 nm and 594 nm for rhodamine B. Light scattering from SUV was reduced by using a 495 nm long-pass filter. Experiments were carried out at room temperature and repeated 5 times, unless mentioned otherwise. The data were corrected for dilution and analyzed using Microcal Origin 7.0 (Microcal Software, Northampton, MA). Fluorophore concentrations were determined with a JASCO V-530 UV spectrophotometer (Easton, MD) using the respective molar extinction coefficients. The same spectrophotometer was used to record absorption spectra of fluorescently labeled lipid vesicles used in RET measurements.

2.5. Calcein release assay

Leakage was studied with SUV loaded with calcein, a dye that self quenches at high concentrations. At a constant concentration of lipid (35 μM), increasing concentrations of dendrimers were added and fluorescence at 520 nm (excited at 494 nm) was measured for a period of time. The percentage of leakage was calculated (with the simplifying

assumption that fluorescence is proportional to extravesicular calcein concentration) using Eq. (1):

$$\text{Percent release} = [(F - F_o) / (F_{max} - F_o)] \times 100, \quad (1)$$

where F_o is the initial fluorescence intensity of calcein-loaded SUV, F is the fluorescence intensity after addition of dendrimers, and F_{max} is the fluorescence intensity after adding 0.1% (w/v) Triton X-100.

2.6. Fluorescence anisotropy

Fluorescence anisotropy was measured with the same fluorometer in the L format with the Glan–Thomson prism polarizers placed in the excitation and emission paths. The cuvette contained 0.2 μM dendrimer, to which SUV were sequentially added up to 400 μM lipid. Data were collected in 5 individual determinations, each with 50 iterations, and fitted with a single hyperbola (Eq. (2)):

$$r = \Delta r_{max} \cdot x / (K_d + x) + r_0, \quad (2)$$

where r is the fluorescence anisotropy, x is the concentration of lipid, Δr_{max} is the maximum change in fluorescence anisotropy at saturating concentration of lipid, K_d is the apparent dissociation constant and r_0 is the initial fluorescence anisotropy. Differences between anisotropy levels were evaluated statistically by one-tailed paired t test with the Prism 4.0a software (GraphPad Software, La Jolla, CA).

2.7. Pyrene aggregation

SUV were prepared with 3% pyrene-PG in the 3:1 egg-PC/egg-PG matrix. Lipid fluorescence was measured in the presence and absence of dendrimers with excitation at 340 nm. The lipid and dendrimer concentrations were 124 μM and 0.5 μM, respectively. The excimer-to-monomer ratio was taken as F475/ F397.

2.8. Resonance energy transfer

RET was measured with the same fluorometer. Aliquots of SUV labeled with 2% rhodamine-PE were sequentially added to fluorescent dendrimer solution. Efficiency (E) of energy transfer between the two fluorophores was calculated using Eq. (3) [21]:

$$E = A_A(\lambda_D) / A_D(\lambda_D)[(I_{AD}(\lambda_D) / I_A(\lambda_D) - 1], \quad (3)$$

where $A_A(\lambda_D)$ is the absorbance of the acceptor at the donor excitation wavelength, $A_D(\lambda_D)$ is the absorbance of the donor at its excitation wavelength, $I_{AD}(\lambda_D)$ is fluorescence intensity of the acceptor excited at the donor wavelength in the presence of the donor, and $I_A(\lambda_D)$ is fluorescence intensity of the acceptor excited at the donor wavelength in the absence of the donor. The distance R between the donor–acceptor pair was calculated from E using Eq.(4) [21]:

$$R = R_o(1/E - 1)^{1/6}, \quad (4)$$

where R_o, the Forster radius, is the distance between the donor and acceptor at which there is a 50% transfer of energy. R_o of the fluorescein/rhodamine B and Oregon green/rhodamine B pairs was taken as 5.2 nm (the orientation factor κ^2 was implicitly assumed to be 2/3).

2.9. Fluorescence quenching

Labeled dendrimers (200 nM) in the NaCl-HEPES buffer were mixed with or without 100 μM of PC/PG (3:1) SUV and fluorescence intensity was measured at increasing concentration of $CoBr_2$ (up to 0.64 mM). The data were analyzed using the modified quenching equation with two quenching constants:

$$F / F_0 = f_1 / (1 + K_{SV1}[Q]) + (1 - f_1) / (1 + K_{SV2}[Q]). \quad (5)$$

Here, F/F_0 is the ratio of quenched and unquenched fluorescence intensities, [Q] is the molar concentration of the quencher and K_{SVi} are the Stern–Volmer quenching constants of fluorophore fractions f_i.

2.10. Light scattering

Light scattering at the right angle was measured in the same fluorometer with both excitation and emission monochromators set to 600 nm (excitation and emission slits were 0.5 and 1.0 mm, respectively). G4 dendrimer (50 or 500 nM) was added to the PC/PG 3:1 SUV (2 μM) suspension in the HEPES buffer, which made the dendrimer/vesicle ratio of about 0.15 and 1.5, respectively. Scattered light intensity was measured in a 1 cm × 1 cm quartz cell in a slow kinetic mode (30 iterations per point). Background light scattering (of the solvent and the instrument) was subtracted. Five independent experiments were used to obtain the average (± standard error) of the dendrimer-induced increase in light scattering.

2.11. Surface tensiometry

Surface pressure of the lipid monolayer at the air-water interface was measured with a μTrough S (Kibron Helsinki, Finland). Stock concentrations (in chloroform) of egg-PC and egg-PG used in these experiments were diluted to 2.5 mg/ml. The trough was filled with 20 ml of NaCl-HEPES buffer and 0.5 μl of egg PC or PC/PG 3:1 were dropped on the surface using a Hamilton syringe. After equilibration, dendrimers were sequentially added into the subphase buffer with a Hamilton syringe in 2 μM increments, and surface pressure at constant area was monitored using the Kibron's software Filmware 2.51.

3. Results

3.1. Fluorescence anisotropy

Dendrimer binding to the membrane was followed by measuring changes in fluorescence anisotropy of the labeled dendrimer. Fluorescence anisotropy of FITC-G1 (200 nM) increased upon binding to PC or PC/PG SUV (Fig. 1). The model of Eq. (2) was used to fit the data. The increased scatter in the PC SUV data might be due to weaker dendrimer binding (compare the K_d values below) and/or longer time required to reach equilibrium in the case of electrically neutral

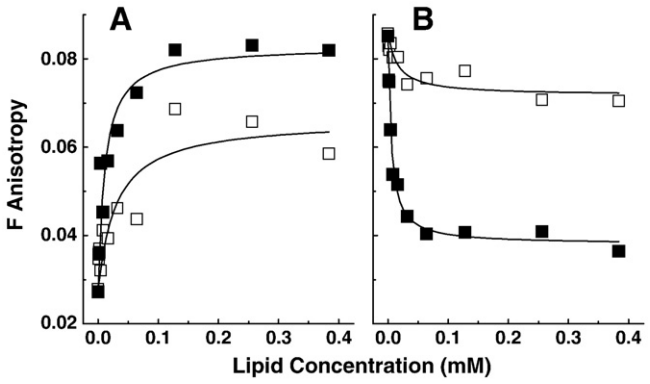

Fig. 1. (A) Interaction of FITC-G1 dendrimer (panel A) and Oregon-green-G4 dendrimer (panel B) with lipid. Open squares, neutral PC SUV; filled squares, negatively charged PC/PG SUV.

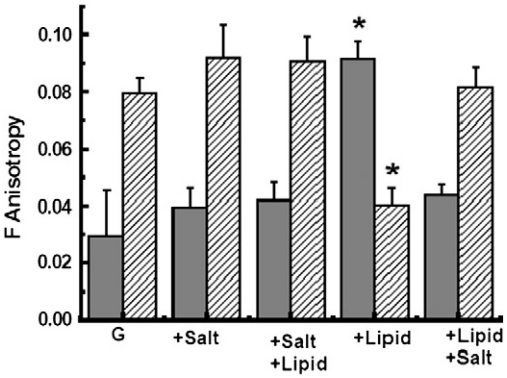

Fig. 2. Effect of 2-M salt on the dendrimer/lipid interaction. Filled bars, G1 dendrimer; cross-hatched bars, G4 dendrimer. Concentration of dendrimers was 0.2 μM; when present, concentration of lipid (in the form of PC/PG SUV) was 120 μM. The experiment was repeated 3 times; an asterisk indicates statistically significant difference ($P<0.05$) between the G and G + lipid samples.

membranes. Quantitative analysis of the data using Eq. (2) gave the values of apparent dissociation constants (K_d) 30 ± 16 μM for PC SUV and 11 ± 3 μM for PC/PG (3:1) SUV. Surprisingly, the Oregon-green label on G4 exhibited a decrease in fluorescence anisotropy upon binding to the vesicles (Fig. 1). Irrespective of the possible physical causes of this behavior, which are discussed in Section 4.1 below, the anisotropy as a function of lipid decreased in a perfectly hyperbolic fashion, which allowed for it being used as a binding parameter in this case, too. Kinetic analysis of the data yielded the following K_d values for G4: 16 ± 7 μM with PC SUV and 5 ± 1 μM with PC/PG (3:1) SUV.

3.2. The effect of salt

Electrostatic interactions, which can be expected due to the high surface charge on the dendrimers, are attenuated by high salt. The addition of 2-M salt did not affect fluorescence anisotropy of G1 by itself (0.03 ± 0.02 vs. 0.04 ± 0.01). When the negatively charged vesicles (PC/PG (3:1) SUV) were added to the dendrimer solution, fluorescence anisotropy increased to 0.09 ± 0.01. When 2-M salt was added to this suspension of dendrimer-lipid complexes, fluorescence anisotropy returned to the initial value observed in the absence of lipid (Fig. 2). The salt-induced changes in fluorescence anisotropy of the larger Oregon-green-labeled G4 dendrimer were similar in absolute value, but, again, opposite in sign (Fig. 2). This indicates

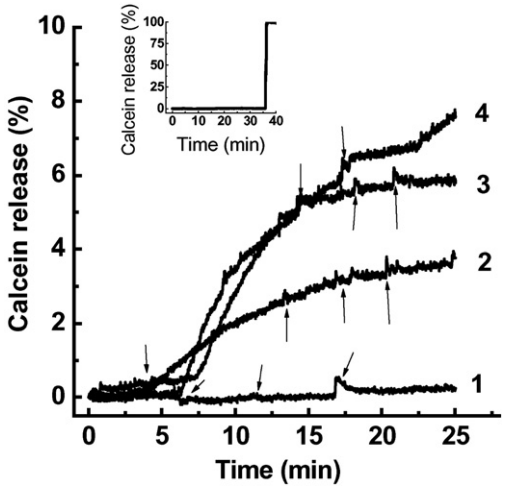

Fig. 3. Dendrimers-induced calcein release from SUV; 1, G1 with neutral SUV; 2, G1 with 25% PG SUV; 3, G4 with neutral SUV; 4, G4 with 25% PG SUV. Arrows indicate additions of 2 μM increments of dendrimers. Inset shows the 100% release upon addition of Triton X-100.

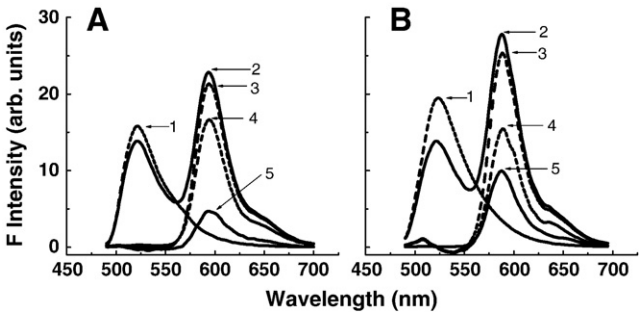

Fig. 4. RET between fluorescently labeled dendrimers (G1 in panel A, G4 in panel B) and rhodamine-labeled lipid. 1, dendrimer excited at 480 nm; 2, after addition of rhodamine-labeled PC/PG SUV; 3, after subtraction of the dendrimer spectrum (No. 1); 4, rhodamine-labeled SUV excited at 480 nm; 5, the RET spectrum (after subtracting No. 4 from No. 3).

that changes in fluorescence anisotropy can be used as binding parameter, irrespective of the direction of dendrimer-induced changes.

3.3. Calcein release

The neutral PC SUV released zero and 6% intravesicular calcein upon binding dendrimers G1 and G4, respectively. Release from the negatively charged PC/PG (3:1) SUV was slightly higher: 4% and 8%, respectively (Fig. 3).

3.4. RET

When rhodamine-labeled negatively charged SUV (egg PC/PG/rhodamine-PE, 73:25:2) were sequentially added to FITC-G1 dendrimer, a decrease in the intensity of FITC fluorescence was observed due to energy transfer to rhodamine B on the membrane surface (Fig. 4). The data allowed for calculation of the average distance between the two fluorophores using Eqs. (3) and (4). With G1 dendrimer the observed energy transfer efficiency (60%) corresponds to a distance of 4.8 ± 0.3 nm, whereas with the larger G4 dendrimer the observed efficiency (99%) implies a distance of 2.0 ± 0.3 nm.

3.5. Fluorescence quenching

A higher binding affinity of the G4 dendrimer compared to G1 can be easily explained by its larger size and a higher surface charge. To get a better insight into the actual binding mechanism we probed aqueous accessibility of the dendrimer fluorophores in the presence and absence of lipid using Co^{2+} as the quencher [36] (Fig. 5). The linearized form of the Stern–Volmer equation did not fit the data well (not shown). Two quenching constants were necessary for a good

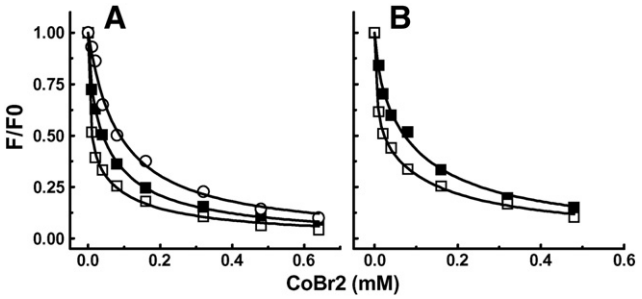

Fig. 5. Quenching of fluorescently labeled dendrimers (G1 in panel A, G4 in panel B) by cobalt bromide in the presence and absence of lipid. Open squares, no lipid; filled squares, 100 μM PC/PG SUV; open circles, in the presence of 1 M salt (filled circle).

Table 1
The effect of lipid on fluorescence quenching of labeled dendrimers.

System	K_{SV1} (mM^{-1})	f_1 (%)	K_{SV2} (mM^{-1})	f_2 (%)	K_{SV} (mM^{-1})
G1	9 ± 2	37	280 ± 70	63	180 ± 40
G1 + PC/PG SUV	12 ± 1	70	190 ± 70	30	65 ± 15
G4	7 ± 1	48	230 ± 60	52	120 ± 30
G4 + PC/PG SUV	8 ± 3	74	100 ± 30	26	36 ± 10

hyperbolic fit, indicating that there were two populations of fluorophores, one that is quenched more readily (a higher quenching constant) than the other (a lower quenching constant). Results are summarized in Table 1. It is most instructive to focus on values of the weighted-average quenching constant K_{SV}. With G1 dendrimer these were 180 ± 40 mM^{-1} and 65 ± 15 mM^{-1} in the absence and presence of lipid, respectively, while for the larger G4 they were 120 ± 30 mM^{-1} and 36 ± 10 mM^{-1}. At high ionic strength (1 M NaCl), quenching was found to follow the linear Stern–Volmer kinetics with a single quenching constant of 13 ± 1 mM^{-1} (Fig. 5A).

3.6. Light scattering

Light scattering of the SUV suspension in the absence and presence of dendrimer was measured in order to test whether the dendrimer can cause vesicle aggregation [35]. In five independent experiments, the addition of 0.5 μM G4 dendrimer to the PC/PG SUV suspension caused a large and rapid increase (by 740 ± 80% within 3 min) in light scattering. A representative trace is shown in Fig. 6. A 10-fold lower concentration of G4 (50 nM) still elicited an increase by 100 ± 5%.

3.7. The effect of membrane fluidity

The effect of membrane fluidity on, and the lateral lipid segregation during, the dendrimer-lipid interaction was studied using the negatively charged egg PC/PG SUV doped with 3% pyrene-PG. Depending on the fluidity of the membrane and on the available free volume, the pyrene moieties at the ends of the labeled lipid's fatty-acyl chains can get close to each other and assume a favorable orientation to form excited dimers–excimers [37]–which fluoresce at longer wavelengths than the monomers. With some simplifying assumptions, an increased rate of excimer formation, that is, increased excimer fluorescence, then indicates decreased distance between the excimer-forming fluorophores. We took the fluorescence ratio F475/F397 as a relative measure of the excimer/monomer ratio. The ratio in the absence of dendrimer was low (0.038)—due to the relatively large average distance between the pyrene moieties at a low concentration in the membrane. Upon the addition of unlabeled G1 dendrimer

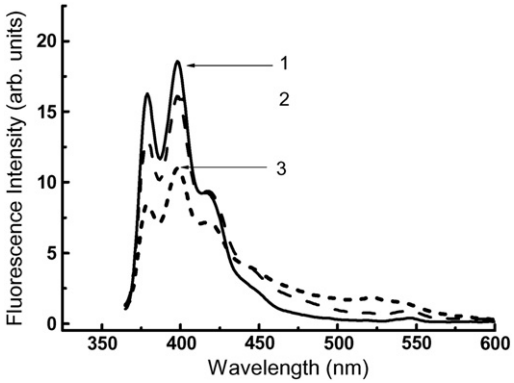

Fig. 7. Dendrimer-induced excimer formation in pyrene-PG/PC/PG (3:75:22) SUV. Spectrum 1, lipid only; spectrum 2, lipid + G1 dendrimers; spectrum 3, lipid + G4 dendrimers.

(300 μM) the ratio increased to 0.111, and with G4 it increased even higher, to 0.214. G4 dendrimer thus showed a twice-greater ability to segregate negatively charged lipids than G1 (Fig. 7). To confirm that we indeed were observing a lateral-diffusion-controlled process we tested the effect of lipid phase (gel vs. liquid crystal) on the dendrimer-lipid interaction (Fig. 8). To that aim we used chemically defined lipids DMPC and DMPG, which exhibit a sharp phase transition in the temperature region around 23 °C [21]. Titrations of DMPC/DMPG (3:1) SUV with dendrimers were carried out at temperatures below (7 °C) and above (37 °C) the phase-transition temperature. For both dendrimers values of K_d were larger in the gel phase than in the liquid-crystal phase: 27 ± 4 μM vs. 14 ± 4 μM for G1 and 58 ± 19 μM vs. 3 ± 1 μM for G4. In addition, the extent of fluorescence anisotropy change was about 3 times smaller below the phase-transition temperature than above. These results indicate that both G1 and G4 dendrimers bind with higher affinity and to a greater extent to fluid membranes in the liquid-crystalline phase than to more rigid membranes in the gel phase. The difference is more pronounced for the larger G4 dendrimer.

3.8. Monolayer surface pressure

The effect of dendrimers on surface pressure of the lipid monolayer, that is, dendrimer penetrating into the monolayer and/or disintegrating it, was tested with the Langmuir trough. We found that upon sequential addition into the monolayer subphase, both G1 and G4 dendrimers increased surface pressure of the negatively charged lipid monolayer, which means that they penetrated below the level of the lipids' hydrophilic head group, but only up to a surface pressure

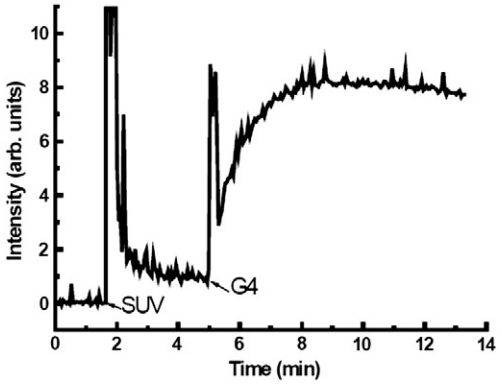

Fig. 6. Dendrimer-induced increase in light scattering of PC/PG (3:1) SUV suspension. Background light scattering by solvent and the instrument was subtracted. Additions of 2 μM lipid and 0.5 μM G4 dendrimer are marked by arrows.

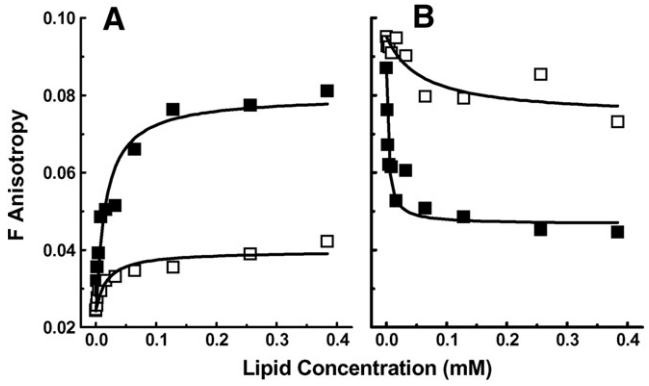

Fig. 8. (A) Effect of lipid phase on the interaction of dendrimers (G1 in panel A, G4 in panel B) with lipid (3:1 DMPC/DMPG SUV). Open squares, gel state at 7 °C; filled squares, liquid crystalline state at 37 °C.

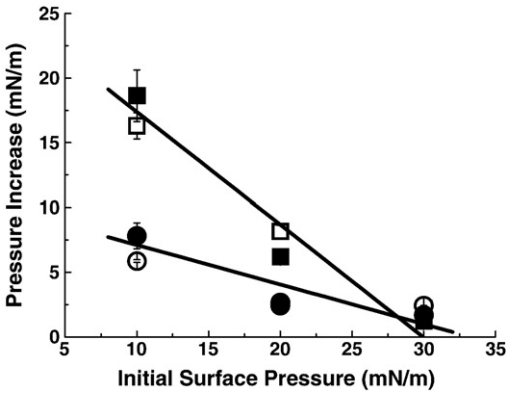

Fig. 9. Effect of initial monolayer surface pressure on the dendrimer-induced pressure increase. Circles, G1 dendrimer; squares, G4 dendrimer; open symbols, PC SUV; filled symbols, PC/PG SUV. Each point is an average of three independent determinations, the error bar is standard error; the lines are linear fits of aggregate data for each dendrimer.

of about 30 mN/m. Above this critical value, which, interestingly, corresponds to the physiologic value in membranes of normal cells, dendrimers did not insert and thus did not elicit any increase in surface pressure (Fig. 9). When the data of each individual titration were plotted as $\Delta\Pi$ vs. Π (not shown), extrapolation of the straight lines to the Π axis yielded the values of critical surface pressure Π_{crit}, above which there was no insertion into the monolayer. As Table 2 documents, values of Π_{crit} strongly depended on initial surface pressure, but the maximum obtainable value, 32.2 ± 0.5 mN/m, did not depend on the nature of either the lipid or the dendrimer.

4. Discussion

The volume and pace of pharmaceutical dendrimer research seems to be on the rise: numerous in situ studies with dendrimers in cells and tissues have been conducted [17,28,29,31], and the first dendrimer-based product appears to be successful in a human clinical trial [38]. Yet, we still have gaps in knowledge of dendrimers' behavior and conformation in the lipid bilayer or, for that matter, even in aqueous solvent. Experiments described in this paper were designed to elucidate some aspects of dendrimer-membrane interactions.

4.1. The lipid-induced changes in dendrimer fluorescence anisotropy

We used changes in dendrimer fluorescence anisotropy to measure binding to the membrane and derive apparent dissociation constants. Our data confirm that PAMAM dendrimers bind more strongly to negatively charged PC/PG membranes than to the neutral PC membranes, which is not surprising. Interestingly, we observed an increase in G1 but a decrease in G4 fluorescence anisotropy. This opposite behavior was rather unexpected, and the reasons for it are not completely clear at present.[2] Possible explanation might be intramolecular electrostatic interactions between the anionic fluorophore and the cationic dendrimer, which is stronger in the larger dendrimer because of the greater surface charge density; this interaction would decrease the fluorophore's rotational diffusion, and thus increase anisotropy, in the larger dendrimer; lipid binding might disrupt this intramolecular interaction and release the fluorophore from the motional restraints with the consequent decrease in fluorescence anisotropy. We will seek an explanation of the phenomenon in future experiments measuring time-resolved fluorescence anisotropy decays at different conditions of pH and ionic strength, which is beyond the scope of the present article. Irrespective of the physical reason for the observed differences, the absolute value of the anisotropy change is used herein as the binding parameter (i.e., the variable that reports the extent of binding), which is justified by the reversibility of dendrimer-induced anisotropy changes, shown in Fig. 2.

Table 2
The effect of initial surface pressure Π_{init} on critical surface pressure Π_{crit} observed in neutral and negatively charged lipid monolayers.

Dendrimer	Lipid	Π_{crit} (mN/m)		
		$\Pi_{init} = 10$ mN/m	$\Pi_{init} = 20$ mN/m	$\Pi_{init} = 30$ mN/m
G1	PC	15.7	21.9	32.1
	PC/PG (3:1)	17.8	23.0	32.9
G4	PC	26.7	28.1	32.1
	PC/PG (3:1)	29.1	26.4	31.8

Throughout our present paper we assumed that the average stoichiometry (1:1) represents the only molecular species present in the sample, which is not correct. When macromolecules or nanoparticles with multiple reactive sites are fluorescently labeled, Poisson distribution dictates that there are always labeled molecules present that have 0, 1, 2, 3, etc., dyes (with decreasing abundance, depending on the aimed dye/molecule stoichiometry). Mullen et al. [39] recently addressed this issue experimentally and theoretically, particularly for the case of PAMAM dendrimers. The question is how the presence of unlabeled, and doubly, triply, etc., labeled dendrimers influences our results and their interpretations. In the first approximation, there is no reason to assume that the unlabeled and labeled dendrimers would bind lipid differently, which means that the K_d determined from the labeled population is the same as for the unlabeled one. The situation is different with dendrimers labeled with multiple dyes. A single binding event would then be interpreted as a multiple change in the fluorescence parameter, the constructed fluorescence curve would be steeper, and the calculated K_d would be lower than the "true" value. We must therefore concede that our kinetic analysis yields lower limits of K_d rather than the "true" values. On the other hand, the dyes' behavior in quenching experiments (discussed in Section 4.4 below) should not depend on whether the fluorophores are on the same dendrimer or not. At any rate, due to the electrostatic repulsion between the negatively charged dyes, no cooperativity is expected during the labeling reaction that would lead to clusters of closely spaced dyes.

4.2. The effect of lipid composition.

Affinity of the cationic PAMAM dendrimers to membranes increased with increasing negative charge in the membrane. Values of apparent dissociation constant (K_d) for both G1 and G4 dendrimers were 3 times lower for vesicles containing 25 mol% negatively charged lipid than for neutral membranes (11 ± 3 μM vs. 30 ± 16 μM for G1 and 5 ± 1 μM vs. 16 ± 7 μM for G4). High salt caused a complete reversal of fluorescence anisotropy changes and hence a complete dissociation of dendrimers from the membrane (Fig. 2). This suggests the electrostatic nature of binding, which implies that only the polar head groups of the lipid and the surface amino groups of the dendrimers are involved in the interaction. At least on the time scale of our experiments (minutes), non-electrostatic forces, such as, e.g., hydrophobic interactions between the inner hydrophobic cores of both the dendrimers and the bilayer did not contribute to the binding. Similar conclusions were reached previously [12,25,40], but recent molecular dynamics simulations of PAMAM dendrimers on a lipid bilayer suggested that hydrophobic forces may play a role in the

[2] Switching from fluorescein to Oregon green in labeling the dendrimers was due to photobleaching concerns in another project in our laboratory, and is incidental to the purposes of this work. Fluorescein and Oregon green are very similar structurally (they only differ in two atoms, with hydrogen replaced by fluorine) and spectroscopically (spectra, lifetime). Therefore the observed differences in the behavior of differentially labeled G1 and G4 dendrimers are ascribed to the nature of dendrimer itself, and not to the properties of the label.

interaction, particularly when the membrane is in the fluid, liquid crystalline state [41,42]. From the molecular dynamics simulations, Kelly et al. [43] calculated the heat (enthalpy) released upon binding of G3 dendrimer to DMPC bilayer as 150 kJ/mol. The Gibbs free energy calculated from the apparent K_d of dendrimer binding to egg PC SUV in this work is substantially lower (27 ± 1 kJ/mol for G4), suggesting a compensatory negative entropic contribution to the free energy of binding, which may come from the local decrease of lipid disorder in fluid phase and from restricted motional freedom within the dendrimer itself. The positive entropic contribution due to the release of water molecules from hydration layers on the membrane and the dendrimer appears to be insufficient to counteract this compensation. The presence of 150 mM NaCl in our experiments would further lower the value of binding free energy when compared to the pure water as solvent. (Kelly et al. used implicit water and a distance-dependent dielectric constant in their simulations, but did not give details on the effective counterion concentration.)

4.3. Membrane disruption

Membrane disruption by low-generation dendrimers *in vitro* was studied using calcein-loaded SUV. We noticed a very minimal but non-negligible membrane damage by the dendrimers used. The G4 dendrimer released about 8% of the dye from PC/PG SUV and about 6% from the neutral PC SUV (Fig. 3), which is in the similar range as the data of Zhang and Smith [23], who used vesicles with different lipid composition. The trend was the same with the G1 dendrimer, but the leakage was even smaller: 4% for PC/PG SUV and zero for PC SUV. Our data confirm previous indications [23,25] that the low-generation dendrimers do not readily permeabilize lipid membranes, in contrast with the high-generation ones [44,45]. It is relevant to note that live cells, with their membrane repair mechanisms, are significantly more impervious to dendrimers than lipid vesicles [28].

4.4. Vesicle aggregation

Cobalt (II) ion is a good quencher of fluorescein-like fluorophores, and we used it to assess accessibility of dendrimer-conjugated fluorophores to the aqueous phase. Unexpectedly, quenching curves revealed that there were two distinct populations of dendrimer-anchored fluorophores in solution. One population was very well quenchable, with a quenching constant K_{SV} in the order of 200 mM^{-1}, and the other was significantly less accessible, with K_{SV} of about 10 mM^{-1} (Table 1). Assuming the value for fluorescence lifetime of about 4 ns for the fluorophores used [46], even the lower of the two quenching constants implies the value of bimolecular quenching constant k_q ($=K_{SV}/\tau$) of 2.5×10^{12} M^{-1} s^{-1}. This is well over the diffusion-controlled limit of 10^{10} M^{-1} s^{-1}, and consequently, it indicates static quenching, that is, formation of quencher-fluorophore complexes. In view of the opposite charges on the quencher and the fluorophore, this is not surprising, albeit the positive charge present both on the quenching ion and the dendrimer surface may complicate the picture. Indeed, it is finding two fluorophore populations in solution (i.e., in the absence of membranes) that is not trivial. We hypothesize that the less quenchable population is comprised of fluorophores that are partially buried (or "snorkeling") under the surface of the dendrimer molecule. Such conformation could be stabilized by a contribution of hydrophobic and/or van der Waals interactions with the dendrimer core. The more quenchable population consists of fluorophores that are kept at the dendrimer surface by intramolecular electrostatic interactions with the surface amino groups. This hypothesis is supported by two observations: (i) the more-quenchable fraction is smaller in G1 (37%) than in G4 (48%), as the smaller dendrimer has lesser surface charge density and it is easier for the fluorophore to "snorkel" under the not very well defined surface of the smaller dendrimer; (ii) the presence of high salt, which attenuates electrostatic interactions, abolishes the higher quenching constant: all fluorophores are quenched with a single constant of 13 mM^{-1} (Fig. 5A). Regardless of the differential localization of the fluorophore within dendrimers in solution (and consequently, differential quenching), another observation is more pertinent to our conclusions. It is the fact that upon lipid binding, values of the quenching constants decrease 3 or 4 times, as best documented by comparing the single numbers of weighted-average K_{SV}: 180 mM^{-1} to 65 mM^{-1} for G1, and 120 mM^{-1} to 36 mM^{-1} for G4 (Table 1). One possible explanation for protection by lipid against fluorescence quenching would be that dendrimers penetrated inside the vesicles, where the fluorophore would become inaccessible to the extravesicular water-soluble quencher. But such interpretation would require that, if a sizeable fraction of fluorophores internalized, the quenching curve asymptotes were significantly different from zero (or that the linearized Stern–Volmer plot showed downward curvature), which our data (Fig. 5) do not indicate. Other authors failed to detect dendrimer internalization with different fluorescence techniques [23]. Therefore we tested an alternative hypothesis to explain the decreased quenching upon binding to lipid—a dendrimer-induced vesicle aggregation. We suggest that positively charged dendrimers, especially the larger ones, become almost completely engulfed by negatively charged lipid membranes, which hinders (but, significantly, does not completely prevent) the access of the cationic quencher to the anionic fluorophore. Membranes of small unilamellar vesicles with the diameter of 25 nm are not very flexible and it is hard to imagine a single vesicle engulfing a relatively large dendrimer molecule (G4 has a diameter of 4.2 nm [27]). Rather, individual dendrimer molecules would recruit and crosslink multiple vesicles. Our light scattering data (Fig. 6) are consistent with dendrimer-induced vesicle aggregation: a marked, almost nine-fold increase in scattering was observed upon the addition of 0.5 μM G4 dendrimer to the suspension of PC/PG SUV. Admittedly, the simple 90° light-scattering measurement is not a robust method, in that it does not reveal molecular details and it can be confounded by vesicle fusion. Nevertheless, it has often been used in aggregation studies [35,47,48]. We prefer to interpret our results in terms of vesicle aggregation rather than fusion for the following reasons. First, because of the non-linear dependence on the scatterer size, the extent of the light scattering increase due to fusion is usually smaller (up to 2-fold [47,48]) than that due to aggregation (3- to 12-fold [35,49]). Second, the observed protection by lipid against fluorescence quenching is consistent with vesicle aggregation; vesicle fusion, which only increases the vesicle size, would have no effect on the membrane-bound dendrimer. Third, low generation dendrimers are not known to be good fusogens: for example, Zhang and Smith [23] only observed limited fusion with G4 PAMAM dendrimers, and Tsogas et al. [50] had to use guanidinylated G4 dendrimers at either high concentration or high guanidinylation level to observe significant fusion of negatively charged vesicles. The fourth, albeit less direct, support for dendrimer-induced vesicle aggregation comes from the RET data. We observed that the average distance between the donor fluorophore on dendrimer and the acceptor in the membrane decreased with the increasing dendrimer size. In the absence of vesicle aggregation, if dendrimers stayed on the surface of individual vesicles, one would expect just the opposite: with increasing dendrimer diameter, its fluorophore would be found, on average, farther and farther from the membrane surface. The lower average distance between the fluorophore and the membrane in the case of G4 vs. G1 thus indicates that the larger dendrimer is on average associated with more lipid vesicles than the smaller dendrimer. As realized previously by Zhang and Smith [23], abnormal hydration (due to steric hindrance) of the rigid, densely packed surface of high-generation dendrimers may contribute to the lowering of the hydration-layer barrier that normally keeps lipid vesicle from aggregating. Indeed, Khopade et al. [51]

observed that the G4 PAMAM dendrimer is capable of forming various aggregate types and mesophases in complex mixtures of lipids.

While our work was in progress, Kelly et al. [52] addressed the issue of stoichiometry and structure of PAMAM dendrimer-lipid complexes using isothermal titration calorimetry, transmission electron microscopy, atomic force microscopy, and dynamic light scattering, in conjunction with molecular dynamic simulations. It is significant that their results obtained by completely different experimental techniques are in a nice agreement with our structural hypotheses formulated above.

4.5. Membrane fluidity

Lateral phase separation, induced by polycationic macromolecules, in anionic membranes of various compositions has been studied by employing changes in the excimer/monomer ratio of pyrene-labeled lipids [21,53–55]. We observed an increase in dendrimer-induced lateral segregation of the anionic lipid PG, which was proportional to the surface charge density on the dendrimer. We extended this observation in experiments designed to study the effect of membrane fluidity on dendrimer binding (Fig. 8), whose results allowed us to conclude that lateral segregation of acidic lipids not only does occur, but in fact lipid lateral mobility seems to be a prerequisite for efficient binding of the dendrimer to the membrane (i.e., it decreases K_d or increases affinity).

Interestingly, Gardikis et al. [56] observed a dendrimer-induced increase in fluidity of neutral membranes and specifically concluded that dendrimers do interact with the lipid alkyl chains. Unfortunately, because of the way they prepared their dendrimer/lipid dispersions (by a technique similar to that of Khopade et al. [51], that is, "forcing" dendrimers into the membrane "manually"—by adding them to the chloroform/lipid solution prior to drying and hydrating the mixture), their conclusion may not readily apply to the case of dendrimers spontaneously interacting with preformed membranes in aqueous suspension. In contrast, Ottaviani et al. [57], who worked with aqueous suspension of vesicles and dendrimers, concluded that dendrimers increased order in lipid acyl chains. Our experiments were not designed to address this issue (that is, how dendrimers affect membrane fluidity), but a possible solution to the discrepant conclusions of Gardikis et al. and Ottaviani et al. is that dendrimers can both increase and decrease membrane fluidity depending on their location with respect to the membrane. If dendrimers only sit on the membrane surface, pushing lipid acyl chains closer together due to the electrostatic interactions between the dendrimer surface groups and lipid head groups, order in the bilayer will increase. If dendrimers penetrate into the hydrophobic core of the bilayer, they will directly disrupt packing of the acyl chains; even though the lipid acyl chains intercalated into the dendrimer core may be immobilized, as shown by Smith et al. [58], global order in the bilayer will decrease due to the random (or rather radial) orientation of the lipid molecules in contact with the dendrimer. Smith et al. [58] used solid-state NMR to show that hydrophobic interactions cause insertion of lipid molecules into the dendrimer core. Dendrimers fully embedded in the bilayer appeared thermodynamically stable for 3 days, which was the duration of their experiments, including sample hydration. However, due to the method of sample preparation (co-dissolving dendrimer with lipid, similarly to Khopade et al. [51] and Gardikis et al. [56]), this work cannot address possible kinetic barriers for dendrimer insertion into the membrane. A notable feature of the system that Smith et al. studied, i.e., multilamellar lipid vesicles, is the extremely small interlamellar space, with hydration level of only 10 water molecules per lipid [58]. This highly non-physiological situation, which does not occur in cellular plasma membranes, was, understandably, necessitated by the employed experimental technique.

4.6. Membrane penetration

The effect of membrane lipid packing and, in particular, of monolayer surface pressure on the interaction of surface-active macromolecules with membranes is routinely studied using the Langmuir trough [59,60]. Holding the area of the lipid monolayer at the air/water interface constant, an increase in surface pressure indicates penetration of the macromolecule from the aqueous "subphase" into the lipid monolayer. A special value of monolayer surface pressure, called the bilayer-monolayer equivalence pressure, was experimentally determined to be between 30.7 and 32.5 mN/m [61]. At this surface pressure molecules bound equally well to the monolayer and the bilayer membrane, and it is therefore assumed that this value, usually taken as 30 mN/m (see, for example, [62]) represents the normal surface pressure in the lipid bilayer membrane. It has been established that membrane surface pressure decreases (or, equivalently, surface tension increases) during mitosis [63].

We found that both G1 and G4 dendrimers incorporate into the monolayer at low surface pressures (Fig. 9), which only are seen in cells undergoing rapid mitotic division and turnover, such as cancer cells or the short-lived cells lining epithelial surface. Our findings thus justify the expectations of dendrimers' use as transcellular drug-delivery vehicles targeting cancer cells or epithelial cells. Negligible dendrimer-induced changes in surface pressure observed at or above 30 mN/m argue against dendrimers' incorporation into, or penetration across, membranes of normal cells, unless one postulates the existence of local or transient regions in the membrane with lower surface pressure that can serve as point of entry. As for the values of critical surface pressure being strongly dependent on the initial pressure Π_i in individual experiments, we offer the following explanation. At a low value of Π_i numerous molecules of dendrimer can find enough room to insert into the monolayer. But with each subsequent addition, dendrimers that already are in the monolayer decrease the latter's negative surface potential and consequently, they decrease the attractive force experienced by dendrimers still in solution. The result would be just what we observed: at low initial pressures dendrimers stop penetrating not because of the limiting value of surface pressure was reached, but rather because of the cessation of the electrostatic force that drives them into the monolayer. At a higher value of Π_i the monolayer surface presumably does not saturate with the positive charge on dendrimers and the limit to dendrimer penetration is determined by molecular packing or surface pressure in the monolayer.

Recently published molecular dynamics simulations of PAMAM dendrimers interacting with bilayers under various degrees of mechanical stress [64] are relevant to our results. Yan and Yu's course-grained simulations indicate qualitative differences between dendrimer/bilayer systems with different surface tension: with an increasing tension (that is, a decreasing surface pressure or an increasing area per lipid molecule) they observed an increased permeation of dendrimers across the membrane and an increased tendency of the membrane to rupture. This is in accord with our conclusion that dendrimers interact stronger with membranes at lower surface pressure.

While our experiments were not intended to detect lipid nonlamellar phases, the suggestion of Zhang and Smith [23] that dendrimers induce formation of inverse hexagonal phase in the membrane is interesting, as it may explain both the vesicle aggregation and the increase in membrane curvature as a result of the presence of dendrimers. The phenomenon deserves further experimental study.

5. Conclusion

We confirmed that lower generation dendrimers bind electrostatically to the lipid membrane while minimally disturbing its ion permeability barrier. Our data suggest that PAMAM dendrimers

induce aggregation of negatively charged lipid vesicle. Two parameters (which are interrelated), namely the physical state of the membrane (gel vs. liquid crystal) and membrane surface pressure, significantly affect dendrimers' binding to lipid vesicles, which should be taken into account in designing dendrimers as drug-delivery vehicles. Our physico-chemical data contribute to theoretical basis for the potential specific use of dendrimers in transcellular epithelial transport and in the delivery of chemotherapeutic agents.

6. Role of the funding source

Financial support was in part provided by a grant from the National Institute of Biomedical Imaging and Bioengineering (R01EB07470) (HG) and a National Institute of General Medical Sciences National Research Service Award Predoctoral Fellowship (F31-GM67278) (KMK). The funding source had no involvement in study design; in the collection, analysis and interpretation of data; in the writing of the report; and in the decision to submit the paper for publication.

References

[1] G.R. Newkome, Z.Q. Yao, G.R. Baker, V.K. Gupta, Cascade molecules: A [27]-arborol, J. Org. Chem. 50 (1985) 2003–2005.
[2] D.A. Tomalia, H. Baker, J.R. Dewald, M. Hall, G. Kallos, S. Martin, J. Roeck, J. Ryder, P. Smith, A new class of polymers: Starburst-dendritic macromolecules, Polym. J. 17 (1985) 117–132.
[3] J. Alper, Rising chemical "stars" could play many roles, Science 251 (1991) 1562–1564.
[4] D.A. Tomalia, A.M. Naylor, W.A. Goddard III, Starburst dendrimers: molecular-level control of size, shape, surface chemistry, topology, and flexibilty from atoms to macroscopic matter, Angew. Chem. Int. Edn. Engl. 29 (1990) 138–175.
[5] R. Esfand, D.A. Tomalia, Poly(amidoamine) (PAMAM) dendrimers: from biomimicry to drug delivery and biomedical applications, Drug Discov. Today 6 (2001) 427–436.
[6] C.L. Jackson, H.D. Chanzy, F.P. Booy, B.J. Drake, D.A. Tomalia, B.J. Bauer, E.J. Amis, Visualization of dendrimer molecules by transmission electron microscopy (TEM): staining methods and Cryo-TEM of vitrified solutions, Macromolecules 31 (1998) 6259–6265.
[7] J.F.G.A. Jansen, E.M.M. de Brabander-van den Berg, E.W. Meijer, Encapsulation of Guest Molecules into a Dendritic Box, Science 266 (1994) 1226–1229.
[8] R. Duncan, The dawning era of polymer therapeutics, Nat. Rev. Drug Discov. 2 (2003) 347–360.
[9] K.M. Kitchens, M.E. El-Sayed, H. Ghandehari, Transepithelial and endothelial transport of poly (amidoamine) dendrimers, Adv. Drug Deliv. Rev. 57 (2005) 2163–2176.
[10] S. Svenson, D.A. Tomalia, Dendrimers in biomedical applications—reflections on the field, Adv. Drug Deliv. Rev. 57 (2005) 2106–2129.
[11] A. Bielinska, J.F. Kukowska-Latallo, J. Johnson, D.A. Tomalia, J.R. Baker Jr., Regulation of in vitro gene expression using antisense oligonucleotides or antisense expression plasmids transfected using starburst PAMAM dendrimers, Nucleic Acids Res. 24 (1996) 2176–2182.
[12] N. Karoonuthaisri, K. Titiyevskiy, J.L. Thomas, Destabilization of fatty-acid-containing liposomes by polyamidoamine dendrimers, Colloid Surf. B Biointerfaces 27 (2003) 365–375.
[13] M.X. Tang, C.T. Redemann, F.C. Szoka Jr., In vitro gene delivery by degraded polyamidoamine dendrimers, Bioconjug. Chem. 7 (1996) 703–714.
[14] M.P. Turunen, M.O. Hiltunen, M. Ruponen, L. Virkamaki, F.C. Szoka Jr., A. Urtti, S. Yla-Herttuala, Efficient adventitial gene delivery to rabbit carotid artery with cationic polymer–plasmid complexes, Gene Ther. 6 (1999) 6–11.
[15] R.F. Barth, D.M. Adams, A.H. Soloway, F. Alam, M.V. Darby, Boronated starburst dendrimer-monoclonal antibody immunoconjugates: evaluation as a potential delivery system for neutron capture therapy, Bioconjug. Chem. 5 (1994) 58–66.
[16] R.X. Zhuo, B. Du, Z.R. Lu, In vitro release of 5-fluorouracil with cyclic core dendritic polymer, J. Control. Release 57 (1999) 249–257.
[17] M. El-Sayed, M. Ginski, C. Rhodes, H. Ghandehari, Transepithelial transport of poly (amidoamine) dendrimers across Caco-2 cell monolayers, J. Control. Release 81 (2002) 355–365.
[18] R. Jevprasesphant, J. Penny, D. Attwood, N.B. McKeown, A. D'Emanuele, Engineering of dendrimer surfaces to enhance transepithelial transport and reduce cytotoxicity, Pharm. Res. 20 (2003) 1543–1550.
[19] K.M. Kitchens, R.B. Kolhatkar, P.W. Swaan, N.D. Eddington, H. Ghandehari, Transport of poly(amidoamine) dendrimers across Caco-2 cell monolayers: influence of size, charge and fluorescent labeling, Pharm. Res. 23 (2006) 2818–2826.
[20] M. Zorko, U. Langel, Cell-penetrating peptides: mechanism and kinetics of cargo delivery, Adv. Drug Deliv. Rev. 57 (2005) 529–545.
[21] V. Tiriveedhi, P. Butko, A Fluorescence spectroscopy study on the interactions of the TAT-PTD peptide with model lipid membranes, Biochemistry 46 (2007) 3888–3895.
[22] J.S. Wadia, S.F. Dowdy, Protein transduction technology, Curr. Opin. Biotechnol. 13 (2002) 52–56.
[23] Z.Y. Zhang, B.D. Smith, High-generation polycationic dendrimers are unusually effective at disrupting anionic vesicles: membrane bending model, Bioconjug. Chem. 11 (2000) 805–814.
[24] A. Joliot, A. Prochiantz, Transduction peptides: from technology to physiology, Nat. Cell Biol. 6 (2004) 189–196.
[25] S. Hong, A.U. Bielinska, A. Mecke, B. Keszler, J.L. Beals, X. Shi, L. Balogh, B.G. Orr, J.R. Baker Jr., M.M. Banaszak Holl, Interaction of poly(amidoamine) dendrimers with supported lipid bilayers and cells: hole formation and the relation to transport, Bioconjug. Chem. 15 (2004) 774–782.
[26] A. Prochiantz, Protein transduction: from physiology to technology and vice versa, Adv. Drug Deliv. Rev. 57 (2005) 491–493.
[27] S. Parimi, T.J. Barnes, C.A. Prestidge, PAMAM dendrimer interactions with supported lipid bilayers: a kinetic and mechanistic investigation, Langmuir 24 (2008) 13532–13539.
[28] S. Parimi, T.J. Barnes, D.F. Callen, C.A. Prestidge, Mechanistic insight into cell growth, internalization, and cytotoxicity of PAMAM dendrimers, Biomacromolecules 11 (2010) 382–389.
[29] R. Duncan, L. Izzo, Dendrimer biocompatibility and toxicity, Adv. Drug Deliv. Rev. 57 (2005) 2215–2237.
[30] J.C. Roberts, M.K. Bhalgat, R.T. Zera, Preliminary biological evaluation of polyamidoamine (PAMAM) Starburst dendrimers, J. Biomed. Mater. Res. 30 (1996) 53–65.
[31] Y. Omidi, J. Barar, Induction of human alveolar epithelial cell growth factor receptors by dendrimeric nanostructures, Int. J. Toxicol. 28 (2009) 113–122.
[32] J.F. Kukowska-Latallo, E. Raczka, A. Quintana, C. Chen, M. Rymaszewski, J.R. Baker Jr., Intravascular and endobronchial DNA delivery to murine lung tissue using a novel, nonviral vector, Hum. Gene Ther. 11 (2000) 1385–1395.
[33] A. Quintana, E. Raczka, L. Piehler, I. Lee, A. Myc, I. Majoros, A.K. Patri, T. Thomas, J. Mule, J.R. Baker Jr., Design and function of a dendrimer-based therapeutic nanodevice targeted to tumor cells through the folate receptor, Pharm. Res. 19 (2002) 1310–1316.
[34] J.P. Kampf, D. Cupp, A.M. Kleinfeld, Different mechanisms of free fatty acid flip-flop and dissociation revealed by temperature and molecular species dependence of transport across lipid vesicles, J. Biol. Chem. 281 (2006) 21566–21574.
[35] D. Meyuhas, S. Nir, D. Lichtenberg, Aggregation of phospholipid vesicles by water-soluble polymers, Biophys. J. 71 (1996) 2602–2612.
[36] P. Butko, F. Huang, M. Pusztai-Carey, W.K. Surewicz, Membrane permeabilization induced by cytolytic delta-endotoxin CytA from Bacillus thuringiensis var. israelensis, Biochemistry 35 (1996) 11355–11360.
[37] J.B. Birks, Photophysics of Aromatic Molecules, Wiley-Interscience, New York, 1970.
[38] V. Gajbhiye, V.K. Palanirajan, R.K. Tekade, N.K. Jain, Dendrimers as therapeutic agents: a systematic review, J. Pharm. Pharmacol. 61 (2009) 989–1003.
[39] D.G. Mullen, A.M. Desai, J.N. Waddell, X.M. Cheng, C.V. Kelly, D.Q. McNerny, I.J. Majoros, J.R. Baker Jr., L.M. Sander, B.G. Orr, M.M. Banaszak Holl, The implications of stochastic synthesis for the conjugation of functional groups to nanoparticles, Bioconjug. Chem. 19 (2008) 1748–1752.
[40] C. Wang, E. Wyn-Jones, J. Sidhu, K.C. Tam, Supramolecular complex induced by the binding of sodium dodecyl sulfate to PAMAM dendrimers, Langmuir 23 (2007) 1635–1639.
[41] H. Lee, R.G. Larson, Multiscale modeling of dendrimers and their interactions with bilayers and polyelectrolytes, Molecules 14 (2009) 423–438.
[42] C.V. Kelly, P.R. Leroueil, B.G. Orr, M.M. Banaszak Holl, I. Andricioaei, Poly (amidoamine) dendrimers on lipid bilayers II: effects of bilayer phase and dendrimer termination, J. Phys. Chem. B 112 (2008) 9346–9353.
[43] C.V. Kelly, P.R. Leroueil, E.K. Nett, J.M. Wereszczynski, J.R. Baker Jr., B.G. Orr, M.M. Banaszak Holl, I. Andricioaei, Poly(amidoamine) dendrimers on lipid bilayers I: free energy and conformation of binding, J. Phys. Chem. B 112 (2008) 9337–9345.
[44] A. Mecke, S. Uppuluri, T.M. Sassanella, D.K. Lee, A. Ramamoorthy, J.R. Baker Jr., B.G. Orr, M.M. Banaszak Holl, Direct observation of lipid bilayer disruption by poly (amidoamine) dendrimers, Chem. Phys. Lipids 132 (2004) 3–14.
[45] A. Mecke, I.J. Majoros, A.K. Patri, J.R. Baker Jr., M.M. Holl, B.G. Orr, Lipid bilayer disruption by polycationic polymers: the roles of size and chemical functional group, Langmuir 21 (2005) 10348–10354.
[46] E. Rusinova, V. Tretyachenko-Ladokhina, O.E. Vele, D.F. Senear, J.B. Alexander Ross, Alexa and Oregon Green dyes as fluorescence anisotropy probes for measuring protein-protein and protein-nucleic acid interactions, Anal. Biochem. 308 (2002) 18–25.
[47] S. Bulut, M.Z. Oskolkova, R. Schweins, H. Wennerstrom, U. Olsson, Fusion of nonionic vesicles, Langmuir 26 (2010) 5421–5427.
[48] B.F. de Arcuri, G.F. Vechetti, R.N. Chehin, F.M. Goni, R.D. Morero, Protein-induced fusion of phospholipid vesicles of heterogeneous sizes, Biochem. Biophys. Res. Commun. 262 (1999) 586–590.
[49] P.I. Lelkes, P. Lazarovici, Pardaxin induces aggregation but not fusion of phosphatidylserine vesicles, FEBS Lett. 230 (1988) 131–136.
[50] I. Tsogas, D. Tsiourvas, G. Nounesis, C.M. Paleos, Modeling cell membrane transport: interaction of guanidinylated poly(propylene imine) dendrimers with a liposomal membrane consisting of phosphate-based lipids, Langmuir 22 (2006) 11322–11328.
[51] A.J. Khopade, D.B. Shenoy, S.A. Khopade, N.K. Jain, Phase structures of a hydrated anionic phospholipid composition containing cationic dendrimers and pegylated lipids, Langmuir 20 (2004) 7368–7373.
[52] C.V. Kelly, M.G. Liroff, L.D. Triplett, P.R. Leroueil, D.G. Mullen, J.M. Wallace, S. Meshinchi, J.R. Baker, B.G. Orr, M.M. Banaszak Holl, Stoichiometry and structure of poly(amidoamine) dendrimer–lipid complexes, ACS Nano 3 (2009) 1886–1896.

[53] H. Zhao, A.C. Rinaldi, A. Di Giulio, M. Simmaco, P.K. Kinnunen, Interactions of the antimicrobial peptides temporins with model biomembranes. Comparison of temporins B and L, Biochemistry 41 (2002) 4425–4436.
[54] M.F. Ottaviani, P. Matteini, M. Brustolon, N.J. Nicholas, J. Turro, S. Jockusch, D.A. Tomalia, Characterization of starburst dendrimers and vesicle solutions and their interactions by CW- and pulsed-EPR, TEM, and dynamic light scattering, J. Phys. Chem. B 102 (1998) 6029–6039.
[55] A. Hinderliter, R.L. Biltonen, P.F. Almeida, Lipid modulation of protein-induced membrane domains as a mechanism for controlling signal transduction, Biochemistry 43 (2004) 7102–7110.
[56] K. Gardikis, S. Hatziantoniou, K. Viras, M. Wagner, C. Demetzos, A DSC and Raman spectroscopy study on the effect of PAMAM dendrimer on DPPC model lipid membranes, Int. J. Pharm. 318 (2006) 118–123.
[57] F.M. Ottaviani, R. Daddi, M. Brustolon, N.J. Turro, D.A. Tomalia, Structural Modifications of DMPC Vesicles upon Interaction with Poly(amidoamine) Dendrimers Studied by CW-Electron Paramagnetic Resonance and Electron Spin — Echo Techniques, Langmuir 15 (1999) 1973–1980.
[58] P.E. Smith, J.R. Brender, U.H. Durr, J. Xu, D.G. Mullen, M.M. Banaszak Holl, A. Ramamoorthy, Solid-state NMR reveals the hydrophobic-core location of poly (amidoamine) dendrimers in biomembranes, J. Am. Chem. Soc. 132 (2010) 8087–8097.
[59] S.R. Dennison, L.H. Morton, K. Brandenburg, F. Harris, D.A. Phoenix, Investigations into the ability of an oblique alpha-helical template to provide the basis for design of an antimicrobial anionic amphiphilic peptide, FEBS J. 273 (2006) 3792–3803.
[60] S. Deshayes, M.C. Morris, G. Divita, F. Heitz, Interactions of primary amphipathic cell penetrating peptides with model membranes: consequences on the mechanisms of intracellular delivery of therapeutics, Curr. Pharm. Des. 11 (2005) 3629–3638.
[61] A. Seelig, Local anesthetics and pressure: a comparison of dibucaine binding to lipid monolayers and bilayers, Biochim. Biophys. Acta 899 (1987) 196–204.
[62] S.R. Dennison, S. Dante, T. Hauss, K. Brandenburg, F. Harris, D.A. Phoenix, Investigations into the membrane interactions of m-calpain domain V, Biophys. J. 88 (2005) 3008–3017.
[63] D. Raucher, M.P. Sheetz, Membrane expansion increases endocytosis rate during mitosis, J. Cell Biol. 144 (1999) 497–506.
[64] L.T. Yan, X. Yu, Enhanced permeability of charged dendrimers across tense lipid bilayer membranes, ACS Nano 3 (2009) 2171–2176.